

Design of New Nano-Catalysts and Digital Basket Reactor for Oxidative Desulfurization of Fuel: Experiments and Modelling

Jasim I. Humadi ^{1,a,*}, Amer T. Nawaf¹, Aysar T. Jarullah ^{2,b}, Mustafa A. Ahmed³,

Shymaa Ali Hameed², Iqbal M. Mujtaba^{4,c}

¹Petroleum and Gas Refinery Engineering Department, College of Petroleum Process Engineering, Tikrit University

²Chemical Engineering Department, College of Engineering, Tikrit University

³Ministry of oil, North Refineries Company, Baiji Refinery, Iraq

⁴Department of Chemical Engineering, Faculty of Engineering & Informatics, University of Bradford, Bradford BD7 1DP, UK

^aEmail: jasim_alhashimi_ppe@tu.edu.iq

^b Email: A.T.Jarullah@tu.edu.iq

^c Email: I.M.Mujtaba@bradford.ac.uk

Abstract

This study was focused on developing a new catalyst using metal oxide (10%Mn) over Nano-activated Carbon (Nano-AC) particles and designing a new reactor (digital basket reactor, DBR) for the sulfur removal from kerosene oil via oxidative desulfurization (ODS). The new homemade Nano-catalyst was prepared by utilizing impregnation process and was characterized by SEM, EDX, BET, and FTIR techniques. The performance of ODS process under moderate operating conditions was significantly enhanced by the application of the new catalyst and the new reactor. The results showed that 94% of the sulfur could be achieved at oxidation temperature of 80 °C, oxidation time of 35 min and agitation rate of 750 rpm. The reactivity of catalyst was examined after four consecutive ODS cycles under the optimal experimental parameters and the used catalyst showed excellent stability based on oxidation efficiency. The spent catalyst was treated by methanol, ethanol and iso-octane solvents for regenerated it, and the

result proved that iso-octane carried out the maximum regeneration performance. An optimization method depending on minimizing the sum of the squared error among the experimental and model predicted data of ODS technology was employed to evaluate the optimal kinetic model parameters of the reaction system. The ODS process model was able to predict the results obtained experimentally for a wide range of conditions very well by absolute average errors < 5%.

Keyword: Desulfurization technology, DBR, MnO₂, Nano-AC-support, Oxidant (H₂O₂)

1. Introduction

The environmental protection agency (EPA) and other agencies for environment protection are continuously updating regulations in relation to sulfur compounds in the derivatives of feedstock (fuels) [1]. Sulfur compounds in the fuels are considered one of the most toxic elements impacting the environmental condition and are regarded as the main undesirable compounds in oil derivatives of product like gasoline, kerosene, and diesel oil due to their repulsive odor, corrosive nature and ability to poison catalysts used in chemical reactions [2-7]. It is a global standard to maintain the sulfur content as low as possible to satisfy stringent environmental regulations. The recently proposed legislations require reducing all types of sulfur compounds like dibenzothiophene (DBT) in the petroleum oil [8]. To improve fuel quality with reduced sulfur content requires deep desulfurization process using moderate process parameters (temperature and pressure). Therefore, ODS technology has received considerable attention because of the moderate operating conditions (safety of process), low cost due to the fact that hydrogen (H₂) is not required in the process as is the case with hydrotreating process for sulfur removal. Operating conditions of oxidative desulfurization process requirement reaction

temperature less than 100 °C, reaction time (60-70) min, low pressure (~1 bar) and several oxidants such as (H_2O_2 , O_2 , air ...etc) can be used [9, 10]. The conventional process called hydrodesulfurization process (HDS) requires severe operating conditions (300-450 °C and 35- 270 bar) for reducing sulfur content in fuels [11].

In the desulfurization via oxidation process, sulfur contaminations can be oxidized to sulfone or sulfoxide employing suitable oxidizing agent and effective catalyst but at moderate parameters (temperature and pressure). sulfone or sulfoxide compounds have high polarity and can be removed by adsorption or extraction processes [12]. In ODS process various kinds of oxidants and catalysts can be employed. These oxidants and catalysts must be prevented olefins or aromatics oxidation in the oil [13]. Therefore, the oxidants kinds employed in oxidation reactions for removal sulfur include air, H_2O_2 , O_2 etc. Several investigations on oxidative desulfurization process proved that the efficiency of sulfur removal in the ODS was improved via various types of catalysts by enhancing the oxidant performance like acetic acid [14], formic acid [15], $\text{Mo}/\text{Al}_2\text{O}_3$ [16], activated carbon [17], polyoxometalate [18], and transition metal oxides [19]. In the feedstock, the sulfur compounds can be categorized into two kinds: heterocycles and non- heterocycles, where the non-heterocycles are classified as R-SH, R-S-R' and R-S-S-R' compounds, while the heterocycles are included of thiophenes (Th) and its derivatives [like dibenzothiophene (DBT)] with one to several aromatic rings [20]. The treatment process of thiophene compound from diesel fuel is very difficult by traditional process requiring severe operating conditions as mentioned above [21]. The traditional process hydrogenated sulfur to H_2S gas and hydrocarbons. Production of environmentally friendly fuel in the conventional process is difficult and required high activity for catalyst and expensive hydrogen in large amount at severe unit operating parameters due to high resistance of sulfur compounds. Thus,

traditional HDS technology is required high cost compared to other technologies [22]. **Nawaf et al. (2019)** studied the performance of high percent of 18% ZnO/ nano-alumina for sulfur elimination from kerosene using air as oxidant via ODS technology. The results explained that the high amount of active components significantly enhanced sulfur elimination due to increasing active sites of used nano catalyst [23]. **Humadi et al. (2022)** studied the performance of nano $\text{MnO}_2/\text{SnO}_2$ catalyst under different loading amount of MnO_2 (0%, 1%, and 5%) in sulfur removal efficiency from kerosene via oxidative-extractive desulfurization technology. The obtained data showed that improving the MnO_2 amount was significantly enhanced the oxidation performance [10]. In this work, high percent (10%) of manganese oxide (MnO_2) as active component over nano-activated carbon (AC) was employed to prepare a new homemade nano-catalyst (10% MnO_2 / Nano-AC) for the first time this enhanced the activity of the designed nano catalyst due to increasing active sites. Oxidative desulfurization (ODS) process was carried out in a novel design of digital basket reactor (DBR) to evaluate the reactivity of the designed catalyst to produce eco-friendly kerosene fuel. The spent catalyst was processed via solvent extractive regeneration (SER) process by using methanol, ethanol, and isooctane solvents. Optimization method was applied to get the optimal parameters for ODS kinetic in DBR. The gPROMS (general **PRO**cess **MO**delling **S**ystem) software was utilized for modeling, simulation and optimization of the process. The optimization problem was solved as a Non-Linear Programming (NLP) problem employing a Successive Quadratic Programming (SQP) method.

2. Material Used and Experimental Design

2.1 Material Application

- **Kerosene fuel**

The kerosene is employed as feedstock in the present experimental study and is obtained from *Salah-Al Deen/Iraq - Baiji - North Refinery*. The main specifications of the kerosene used in the process are: Density at 15.6 °C is 0.7845 g/cm³, AIP is 48.8, Dr. test +ve RSH, Flash point is 52 °C, Color +12 and sulfur content is 543 ppm.

- **Manganese acetate Mn (CH₃COO)₂·4H₂O**

Mn (CH₃COO)₂·4H₂O salt was used as a source for active metal oxide for the synthesis catalyst and provided from Sigma Aldrich Company (purity of 99.7%). Active salt material was dissolved in deionized water provided locally.

- **Dibenzothiophene (DBT)**

Dibenzothiophene (DBT) was provided from Aldrich (purity >98%) and employed as model sulfur compound. DBT used in evaluating the activity of the new oxidative desulfurization technology in eliminating harmful sulfur compounds.

- **Support Materials (Activated carbon-Nano-Particles)**

Commercial support materials were provided by the Alpha Chemika Company, India and were utilized in preparation of the new nano-catalysts. The main specifications of the support (Activated carbon-Nano-Particles) used in the process are: Specific surface area (BET=908.88m²g⁻¹), total pore volume ($\rho/\rho_0=990$) 0.5125 cm³g⁻¹ and mean pore diameter is 2.2554 nm.

- **Hydrogen Peroxide (30%H₂O₂)**

H₂O₂ was provided by Sigma Aldrich Company (purity > 99.99%) and employed as oxidant material for converting DBT to corresponding oxidized compounds.

- **Solvents for SER process**

CH₃OH, C₂H₅OH and (CH₃)₃CCH₂CH(CH₃)₂ were used for regeneration process of the new nanocatalyst. Table S1 showed the characteristics of these solvents.

2.2. Incipient Wetness Impregnation (IWI) Process

Preparation of homemade catalyst via Incipient Wetness Impregnation (IWI) [20] method has been employed for ODS reactions. In the first step, the support (AC-activated carbon) is dried to remove any impurities before using it in IWI process. 5g active compound of manganese acetate (Mn(CH₃COO)₂·4H₂O) is dissolved in 55 ml deionized water employing a magnetic stirrer at 450 rpm for 1.5 hr. The solution is filtered for removal all impurities. 15 g of the support (AC) is used to prepare the nano catalyst. IWI method is employed by slowly addition for the active compound (Mn(CH₃COO)₂·4H₂O) solution including the active metals for loading on the catalystsupport and making sure the dispersion of active materials over the support. The mixture isputted in the oven under 110 °C overnight for drying process. After that, the catalyst is calcined under 560 °C for 1.5 hr under N₂ gas (99.99% purity) condition under a heating rate of 5 °C /min. The calcination carried out in the tubular furnace for converting metal salts into metal oxide which loaded on AC support. Calcination of the produced material in the tubular furnace is achieved based the following producer: initially the dried materials are heated at 150 °C for 1.5hr in the tubular furnace for removing any remainder moisture. After that, the calcinationtemperature is increased up to 350 °C for 2 hr to obtain on gradual calcination process and avoid cracking by rapid heating. Finally, the materials are calcined at 560 °C for 1.5 hr to convert Mn salt into MnO₂ and synthesis the novel (10%MnO₂/Nano-AC-support). Figure 1 shows the process schematically.

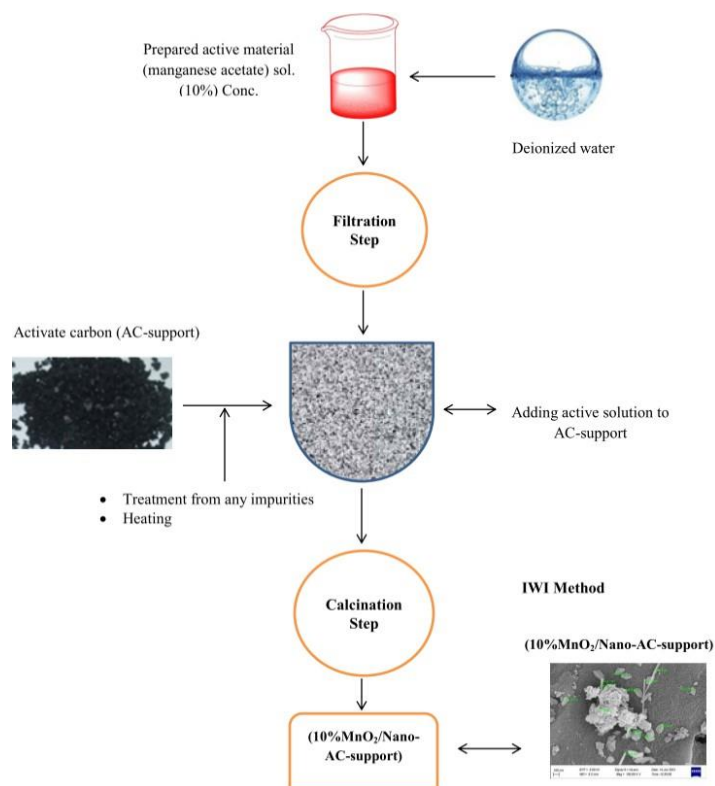


Figure 1: Nano-catalyst designed with metal oxide (manganese acetate $\text{Mn}(\text{CH}_3\text{COO})_2 \cdot 4\text{H}_2\text{O}$)

2.3. Characterization of nanocatalyst

The surface area for AC and the designed Nano-Catalyst ($10\%\text{MnO}_2/\text{AC}$) was examined via BET (Brunauer-Emmett-Teller) test. BET was achieved at the Advanced Materials Research Center and Nanotechnology / Baghdad/ Iraq. The surface area of Nano- AC and $10\%\text{MnO}_2/\text{AC}$ resulted after 24 hr with crystallization temperature of $85\text{ }^\circ\text{C}$. The nano- Catalyst surface morphology of ($10\%\text{MnO}_2/\text{AC}$) catalyst was examined via employing scanning electron microscopy (SEM) (Zeiss-EM10C-100 KV). Fourier Transform Infra-Red (FTIR) of the Nano catalyst was examined by Nicolet 6700 spectrometer (FTIR 8400S/ Shimadzu/ Japan) at the Advanced Materials Research Center and Nanotechnology (Iraq). TGA were tested at Petroleum Research and Development Center (PRDC) laboratory to examine the mass loss of catalyst when the temperature enhanced. 12 mg of the sample was tested and the temperature rate via $3\text{ }^\circ\text{C}/\text{min}$ was increased up to $900\text{ }^\circ\text{C}$.

2.4. Experimental Procedure

- **Design of Basket Reactor (DBR)**

Design of digital basket Reactor DBR was carried out in the College of Petroleum Process Engineering, Tikrit University which provides high dispersion of catalyst in oil and has the best mass transfer characteristics in the ODS technology. The design of such reactor contains electrical digital mixer with speed range from (0-5000) rpm, rod length of 35 cm with four basket impellers at the end of the rod (basket dimension: length 1cm, depth 1 cm and 1cm width). These baskets were manufactured in a novel design to hold nano-catalyst. Such baskets were contained circular holes that distributed equally over the metal surface in a hexagonal manner for increasing the mixing channels in the catalyst and the reactor, leading to increase the conversion process within the path (fuel, catalyst, and oxidizing agent). Baffles were designed on the wall of the reactor to prevent stagnant zone in the reactor and to increase the mixing process of different materials. The volume of the reactor is 250 mL and manufactures using stainless steel materials which includes of four baffles (height 10 cm and width 1.5-1.8 cm). Baffles are installed in equal dimensions shape on the internal surface of the DBR (about 38 cm gap between the baffles) with a protrusion of 2.5 cm with each baffle. The outside of the DBR is insulated via woolen material and is provided with power electrically employing at 5000 rev/min and can operate at severe conditions (temperature > 1000 °C). The experimental setup for the new design of DBR is shown in Figure 2. The specifications of the DBR are explained in Table 1.

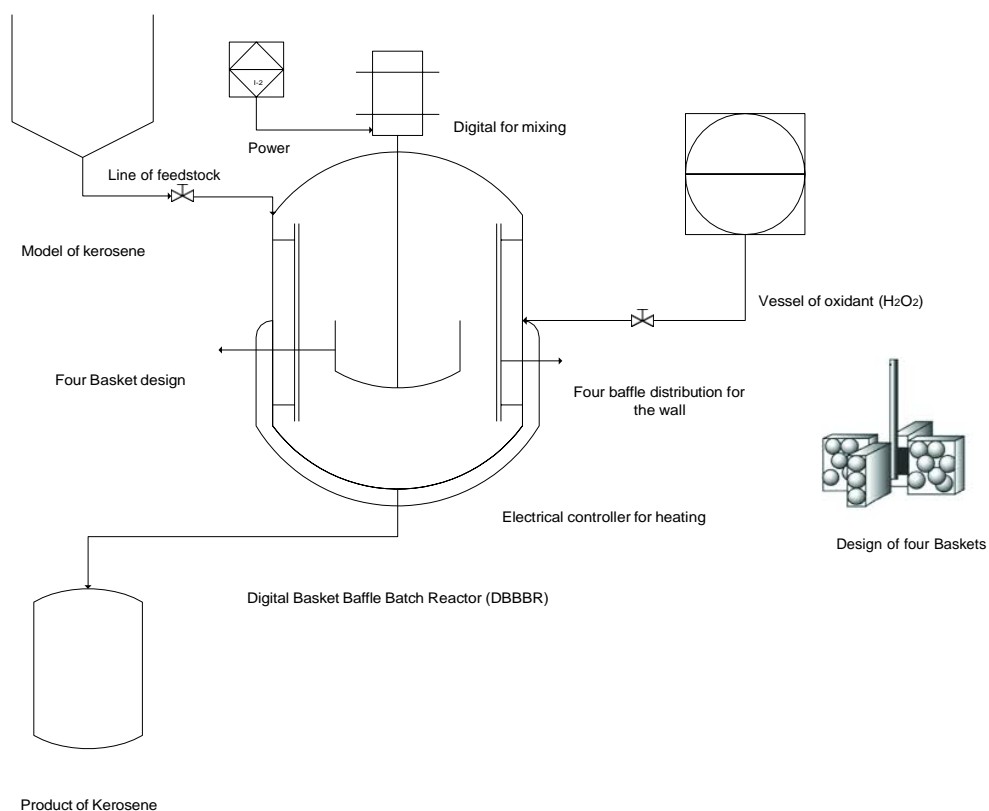


Figure 2: Schematic observation of the digital basket reactor DBR system

Table1: Specification of DBR system

No	Description	Specification
1.	Dimension of reactor (Stainless steel)	D= 8cm , H=10cm
2.	Length of the rod	35 cm
3.	Dimension of basket	H=1cm, L=1cm & W=1cm
4.	Impeller type	Four basket impeller
5.	Impeller diameter	90.0 mm
6.	Batch reactor	Batch made of glass (200.0 mL)
7.	Baffle	4, distributed along the wall of the reactor (height 8cm)
8.	Preheater	Electrical heater
9.	Insulator material	Glass wool

- **Oxidative Desulfurization (ODS) Process in DBR**

For evaluating the performance of the new designed catalyst in the new designed reactor (DBR), kerosene (feedstock) is used. Dibenzothiophene (DBT), as a model sulfur compound, was injected in the kerosene with a total S content of 543 ppm as initial sulfur concentration of the feedstock. In the digital basket reactor, oxidative desulfurization reaction takes place between the model kerosene (feed) and hydrogen peroxide (H_2O_2) (oxidant). In the ODS process, 100 ml of kerosene is feed for each experiment to achieve the oxidative desulfurization reaction. The amount of oil to oxidant (hydrogen peroxide (H_2O_2)) was 25 and all experiments were carried out at constant pressure (1 atm) with 5g of the catalyst. The designed catalyst (Mn/AC) is charged into the basket reactor containing the model kerosene and each basket having 1.25 g of the catalyst. A moderate reaction temperature of 40, 60, 80 and 100 °C with reaction time of 15, 25, 35 and 40 min and magnetic stirrer speed of 250, 500, 750 and 1000 rpm were used. During the chemical reactions, gases are evaporated which are condensed in the condenser. The produced kerosene fuel samples are tested via X-ray diffraction instrument according to ASTM D7039 method for determining the sulfur content using the facilities at Sammraa Power Station Laboratories/Ministry of Electricity-Iraq. Each experimental run are repeated twice and the average results have been taken into accounts for each run with maximum deviation of 2% among all runs.

- **Regeneration of the spent catalyst**

The reactivity of new nano 10% MnO_2/AC catalyst was examined after four ODS cycles under the best experimental parameters that carried out maximum DBT removal. After ODS, the produced materials were subjected for cooling and centrifuging for separating nano catalyst, oil and aqueous phases.

The SER technique was used to regenerate the used nano catalyst. DBT were removed from the used catalyst in a (SER) using iso-octane, ethanol, and methanol. 1 gram of used nano catalyst was shaken in the suspension for 65 minutes at 65 °C using approximately 15 mL of the solvent. The cleaned nano catalyst was filtered before being dried at 115 °C for 12 h.

3. Results and Discussion

3.1 Characterization of the Designed Nano-Catalyst (MnO₂/AC)

3.1.1 Surface Area

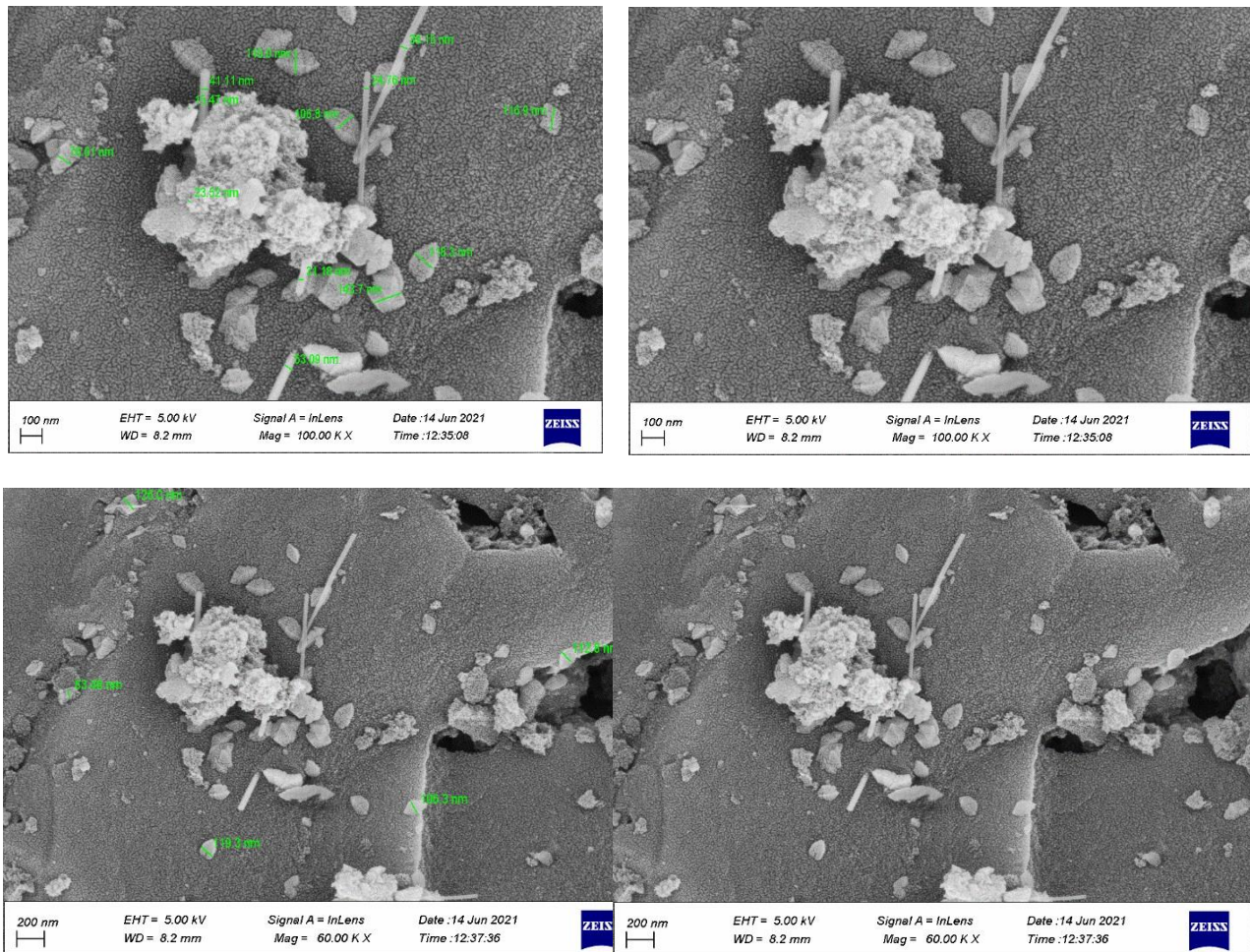
. The surface area of Nano- AC and 10%Mn MnO₂/AC catalysts were explained in Table 2. In the ODS process, the physical and chemical characteristics of the designed catalyst (10%MnO₂/AC), the specific surface area and pore volume are effected dramatically on the ODS performance. In Table 2, the BET data observed that of the designed nano catalyst has decreased after loading 10%MnO₂ on AC. Reduction of the value of the surface area after loading the metal oxides could be returned to the deposition of MnO₂ in the pores of AC leading to blockage and interference in nitrogen diffusion [10]. Although, surface area data are remain in the acceptable range in comparing to the values of active metal oxides on its own.

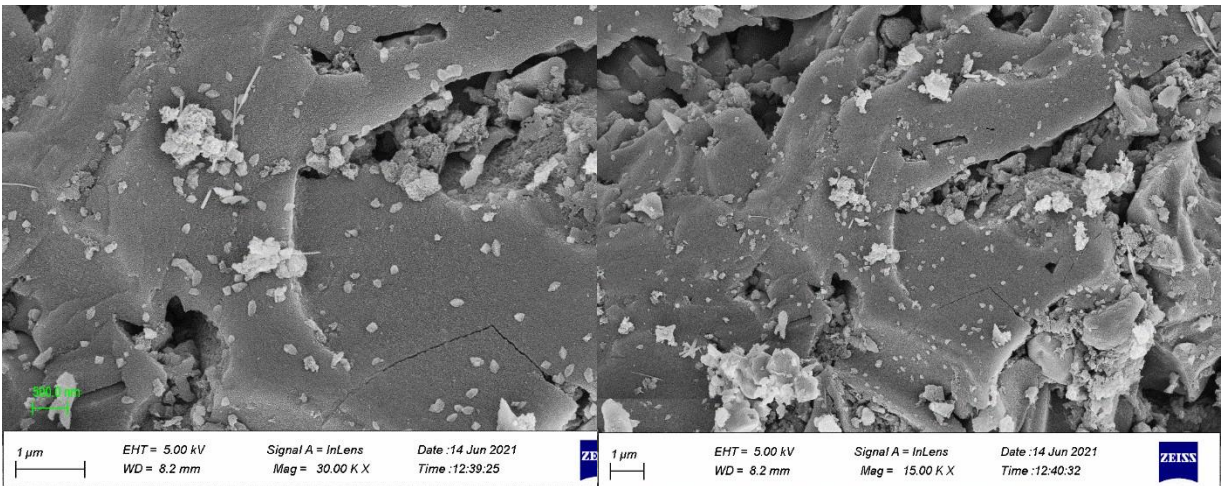
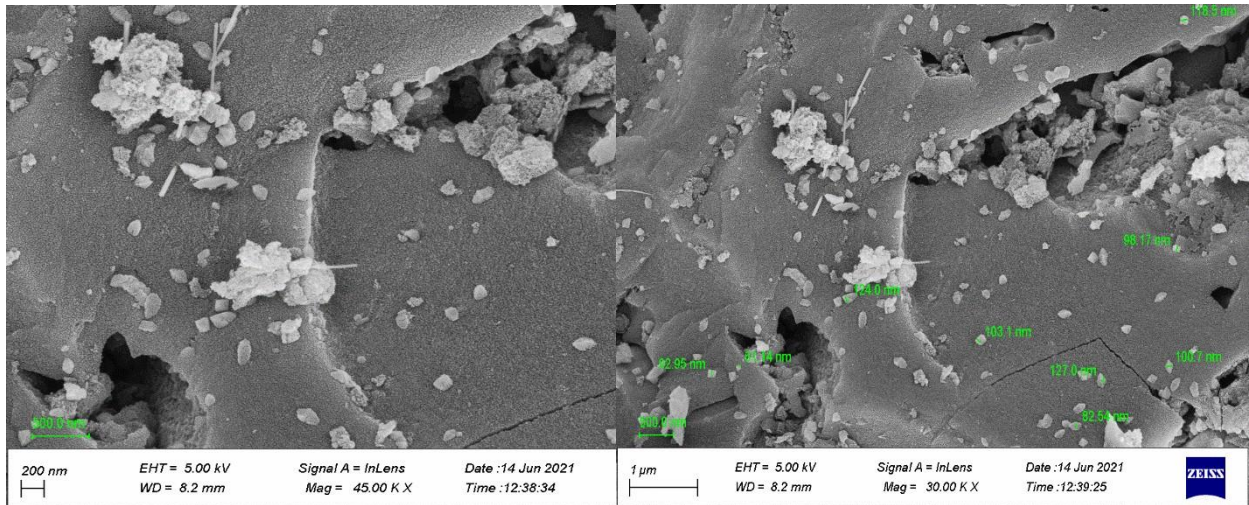
Table 2: Property for support and Nano-catalyst prepared

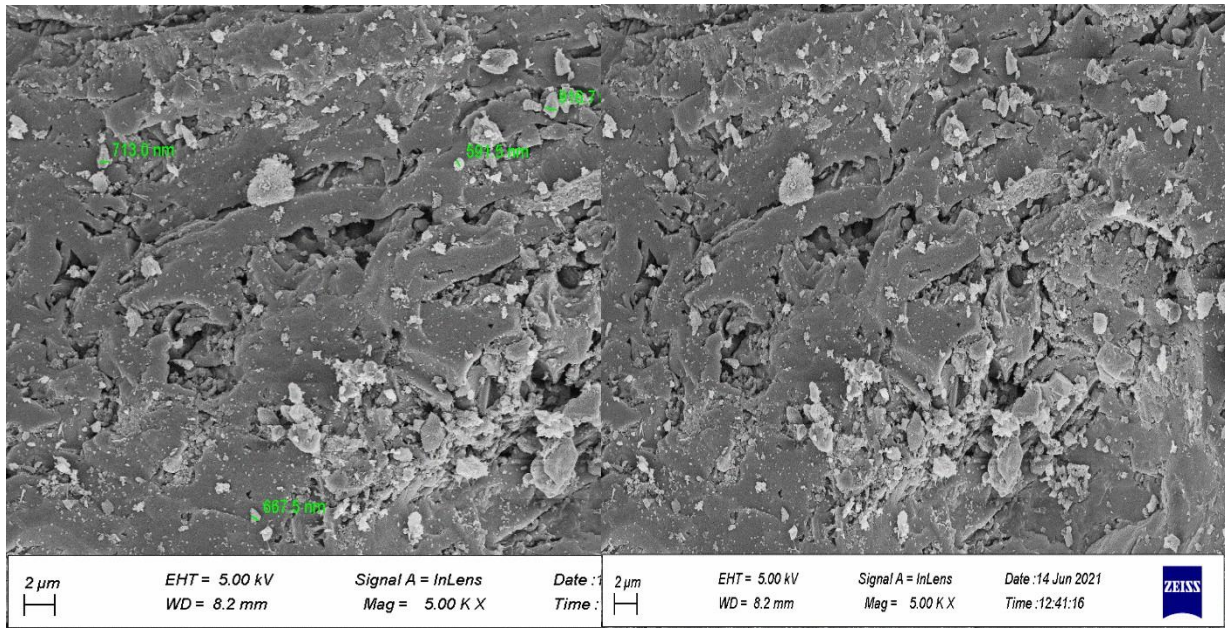
Property	Support (AC)	Catalyst (10%MnO ₂ /AC)
BET	908.88 (m ² g ⁻¹)	707.37(m ² g ⁻¹)
Total pore volume ($p/p_0 = 0.9900$)	0.5125 (cm ³ g ⁻¹)	0.4536(cm ³ g ⁻¹)
Mean pore diameter	2.2554 (nm)	2.4183(nm)

3.2.1 Morphology and elemental analysis of the catalyst prepared (AC/MnO₂-10%)

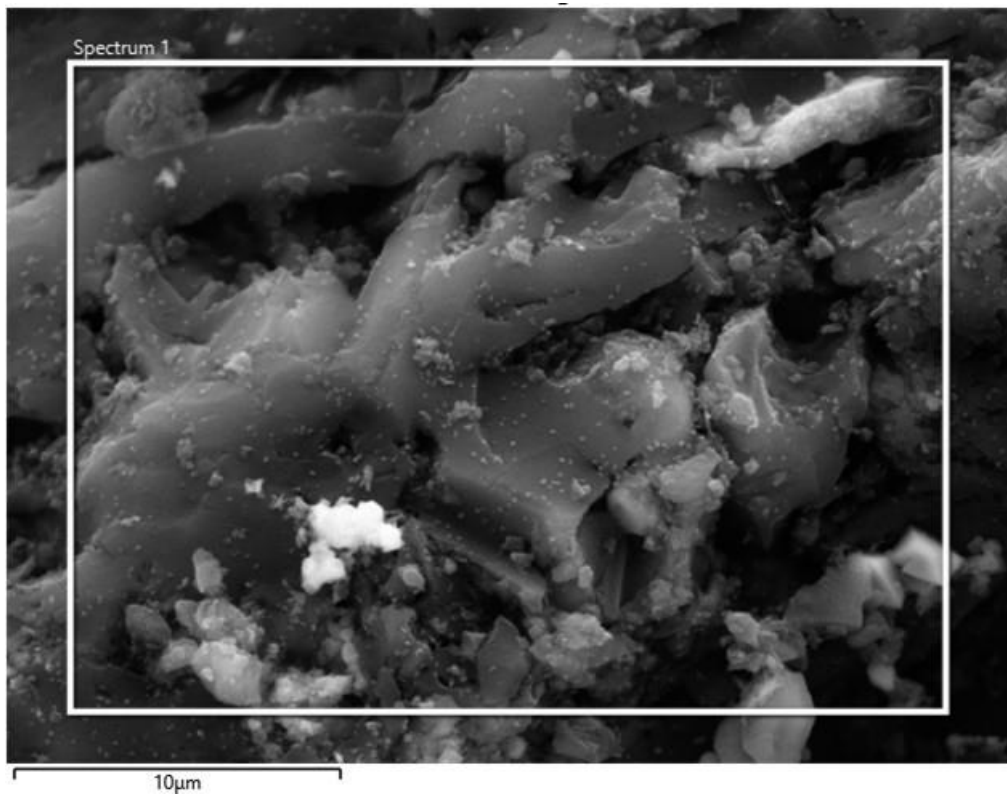
The SEM test results of the characterization of designed nano-catalyst (10% MnO₂/AC) (illustrated in Figure 3) show the dispersion of MnO₂ in the surface of activated carbon. An excellent distribution of MnO₂ over AC surface is noticed (Figure 3a) where the metal is observed in the white regions and AC by dark regions. The EDX analysis (Fig. 3b) clearly shows the composition of the composite elements. The compositions were as follow: 52.74%, 37.04 % and 10.22% for C, O and Mn elements. The data of atomic ratio suggests remarkably presence of other manganese oxides rather than just MnO and such behavior can be inferred also from the FTIR data.

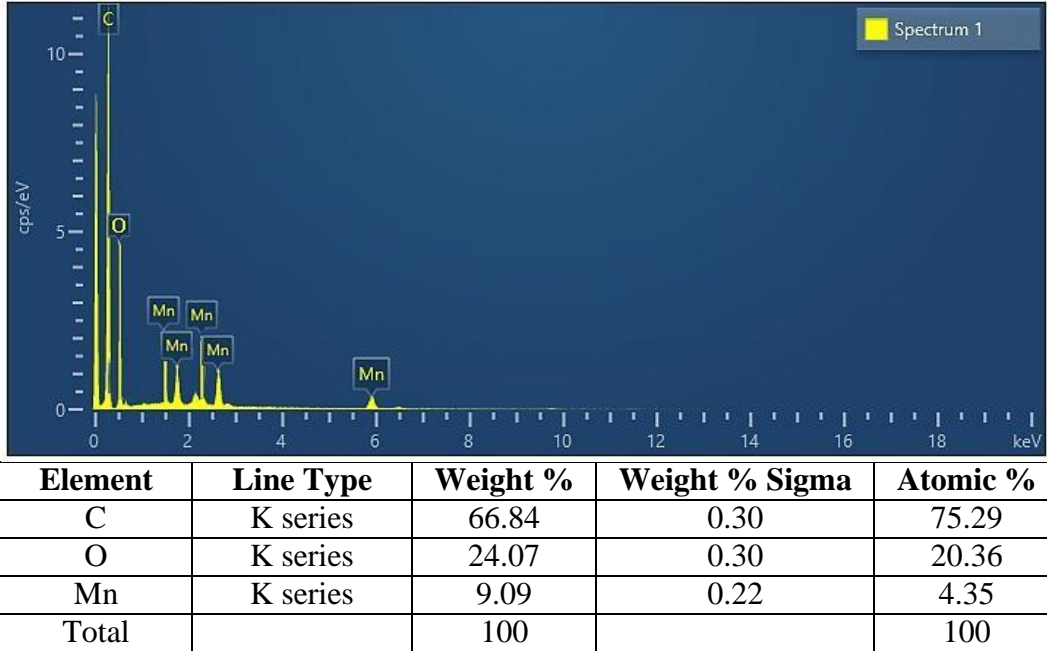






(A)





(B)

Figure 3: (A) SEM images of nano-activated impregnated with manganese oxide 10% MnO₂/Nano-AC-support (B) EDX for oxide 10% MnO₂/Nano-AC-support

3.1.2 FTIR Test

Figure 4 displays the functional groups on Nano-10% MnO₂/AC based on FTIR measurements. While the bands at 2964.39 cm⁻¹ can be referred to as the aliphatic C-H stretching vibration of CH, CH₂, and CH₃, the band at around 3442.70 cm⁻¹ can be referred to as the O-H stretching vibration of hydroxyl groups [24]. The carboxyl group and carbonyl group may be traced back to the band at roughly 1708.18 cm⁻¹ and 1627.81 cm⁻¹. The O-H bending vibration is visible in the absorption band at 1122.49 cm⁻¹, whereas the bands at roughly 673 cm⁻¹ and 525 cm⁻¹ may be traced back to the Mn-O and Mn-O-Mn stretching vibrations, respectively, which demonstrate the existence of MnO₂ on the AC surface [25]. between 2177 and 1870 cm⁻¹, 1870 and 1700 cm⁻¹, and 1708.18 and 1598 cm⁻¹ for the terminal Mn-C=O band. These findings can be related to the functional groups on the 10% MnO₂/AC surface, which are incredibly helpful for the adsorption of sulfur from oil.

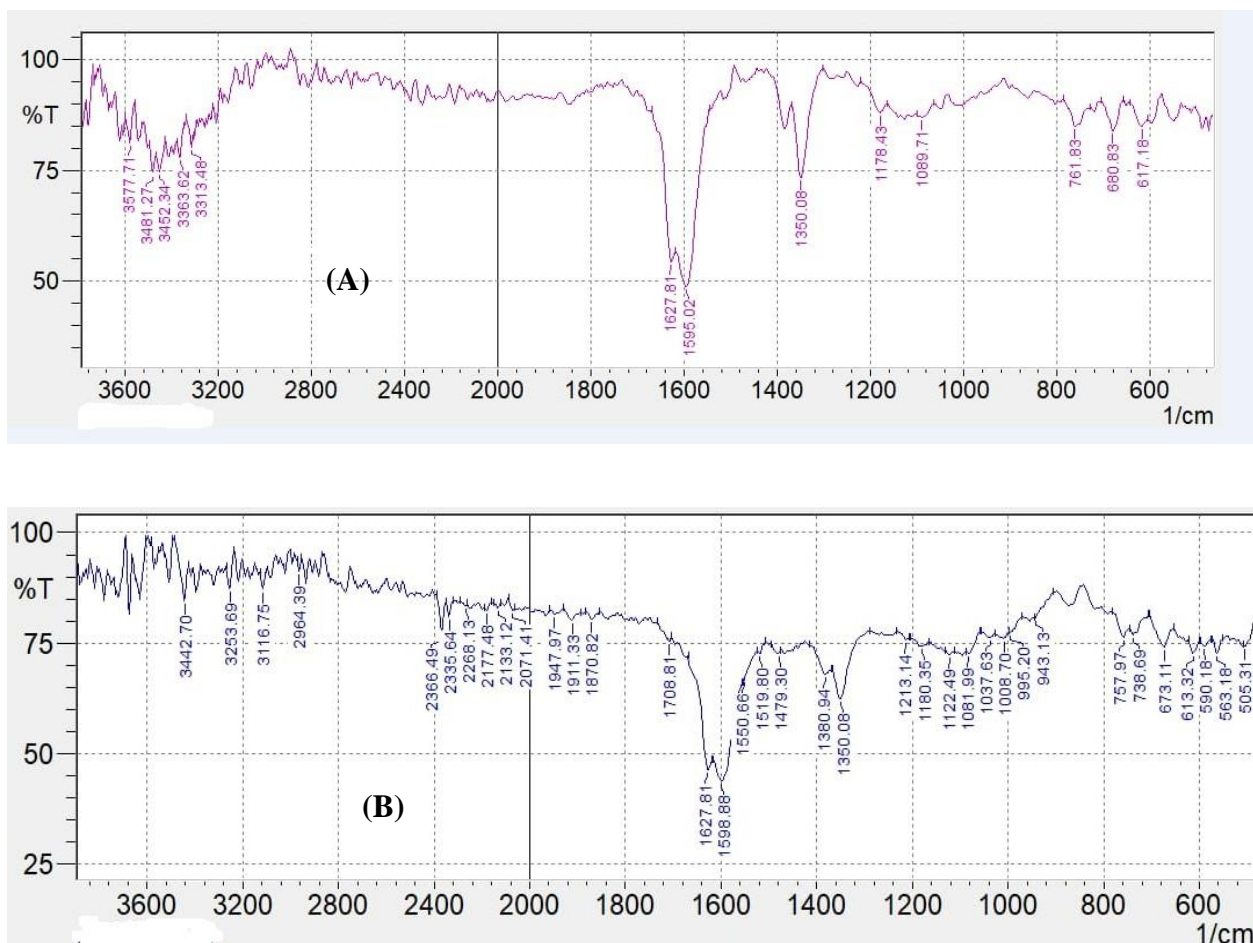
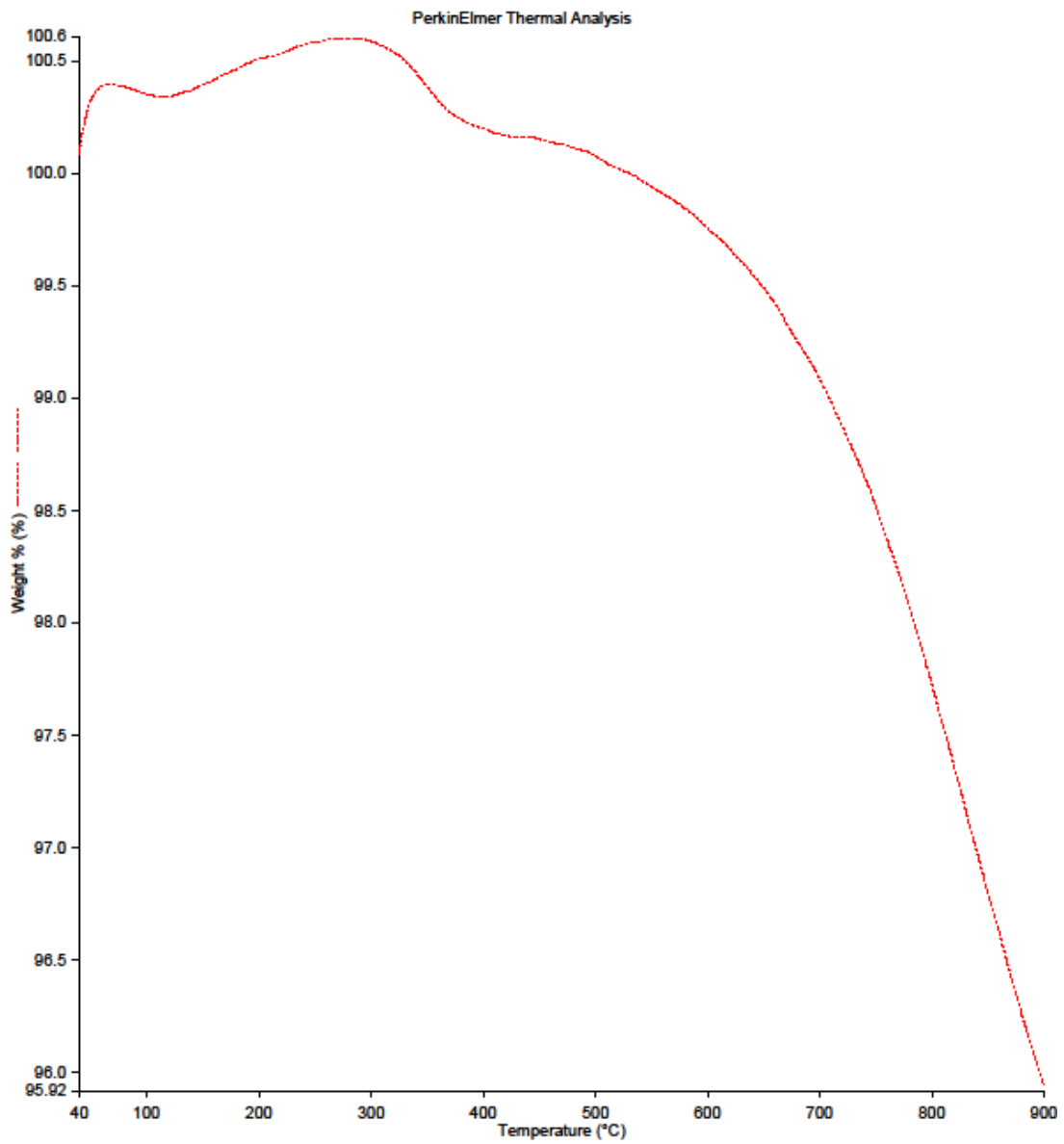


Figure 4: FTIR of the designed Nano-catalysts **(A)** AC-activated carbon **(B)** 10%MnO₂/Nano-AC-support

3.1.3 Thermal Gravimetric Analysis (TGA)

The percentage loss of weight through TGA test for the prepared 10%MnO₂/Nano-AC is shown in Figure 5. As explained in Figure, there is no mass loss in the first region approximately from 40 to 450 °C. After that, the second region from 450 to 900 °C is showed the highest mass loss which represent of 5.08% mass loss. This is most probably owing to the moisture evaporated by the sample during heating. Also, this percent can be attributed to the decomposition of chemical bonded water, hemicellulose, cellulose and lignin to carbon [26-29].

Filename: C:\Program Files\PerkinElme...225ms-7.stad
Operator ID:
Sample ID:
Sample Weight: 5.450 mg
Comment:



1) Hold for 1.0 min at 40.00°C 2) Heat from 40.00°C to 900.00°C at 20.00°C/min

Figure 5: Results of TGA for MAC

3.3 Effect of experimental parameters on ODS within DBR

3.3.1 Effect of Magnetic Stirrer Speed

The sulfur eliminating during the desulfurization via oxidation technology based on the designed Nano-catalyst (10% MnO_2/AC) is reported in the Figure 6. The influence of speed of the stirrer at several reaction temperatures and reaction of time are noted. From these Figures, it can be noticed that the effect of speed from 250 to 1000 rpm leads to increasing conversion of sulfur content of kerosene (feedstock) [30]. The impact of speed of mixing has shown high performance for distribution of the nano-catalyst and giving significant performance toward the ODS reactions employing hydrogen peroxide (H_2O_2) as oxidizing agent. Increasing the speed of mixing increases the conversion of sulfur from 51.2% to 61.32% for reaction time of 45 min, reaction temperature of 40 °C and oil/oxidant 25 as shown in the Figure 6 (a). Changing the speed of mixing in the DBR from 250 to 1000 rpm shows improvement of conversion from 72.87% to 93.22% for oxidation time of 35 min and oxidation temperature of 100 °C (Figure 6d). The novel basket design of the reactor gave more distribution of the catalyst in all parts of the reactor. The highest removal of sulfur content was (94.149%) under the following experimental parameters: oxidation time 35 min, oxidation temperature 80 °C and speed of mixing 750 rpm as explained in Figure 6c. This behavior can be attributed to the surface and porosity of the Nano-catalyst (10% MnO_2/AC -support) that consider a basic role in the sulfur elimination technology.

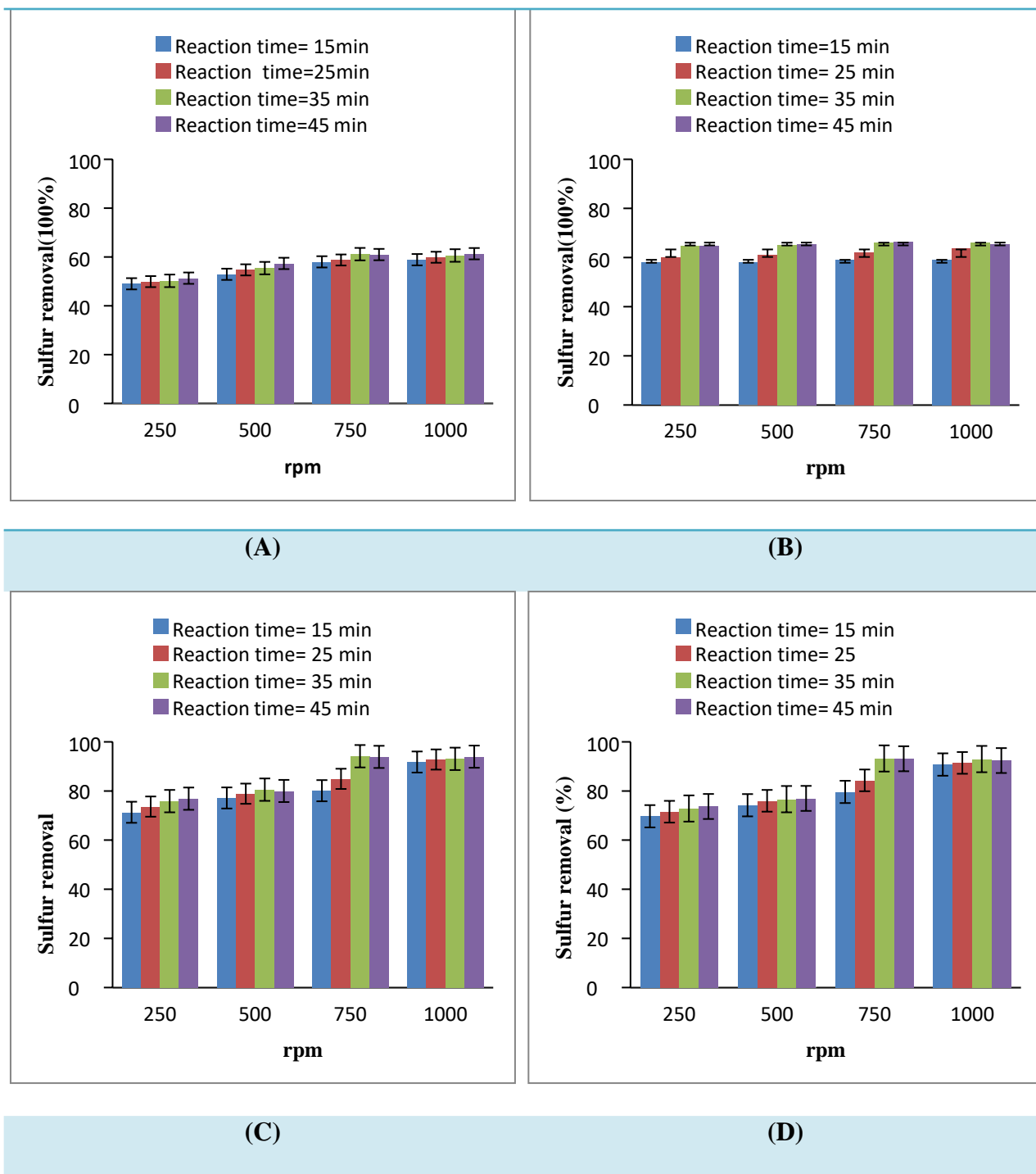


Figure 6: Effect of increasing of speed of mixing (rpm) on the ODS process at A) 40 °C, B) 60 °C, C) 80 °C and D)100 °C, at different reaction time

3.3.2 Effect of Oxidation Time

The impact of digital basket reactor (DBR) time on the removal of sulfur via ODS process using the designed catalyst (10%-MnO₂/AC) are shown in Figure 7 at various experimental parameters. The impact of oxidation time on DBT elimination via ODS technology was examined at 15 min, 25 min, 35 min and 45 min. The results show that enhance in the DBT removal is linked to the oxidation time to a certain extent. This can be returned to the interaction between DBT and H₂O₂ to generate sulfoxide or sulfones which improve as reaction time increases. Also, the results show that the sulfur removing improves with enhancing reaction time, as enhancing contact time between the reactants [31, 32], H₂O₂ improve the DBT and O₂ molecules transferred in the catalyst pores. In Figure 7, the removal of sulfur improves from 59% to 61.32% when the oxidation time enhances from 15 to 45 min at reaction temperature of 40 °C and from 64.89% to 65.56% at 60 °C, from 91.78% to 93.97% at 80 °C and the highest removal of sulfur (from 90.76% to 92.39%) has been obtained at 100 °C. In all these cases, the speed of mixing was 1000rpm.

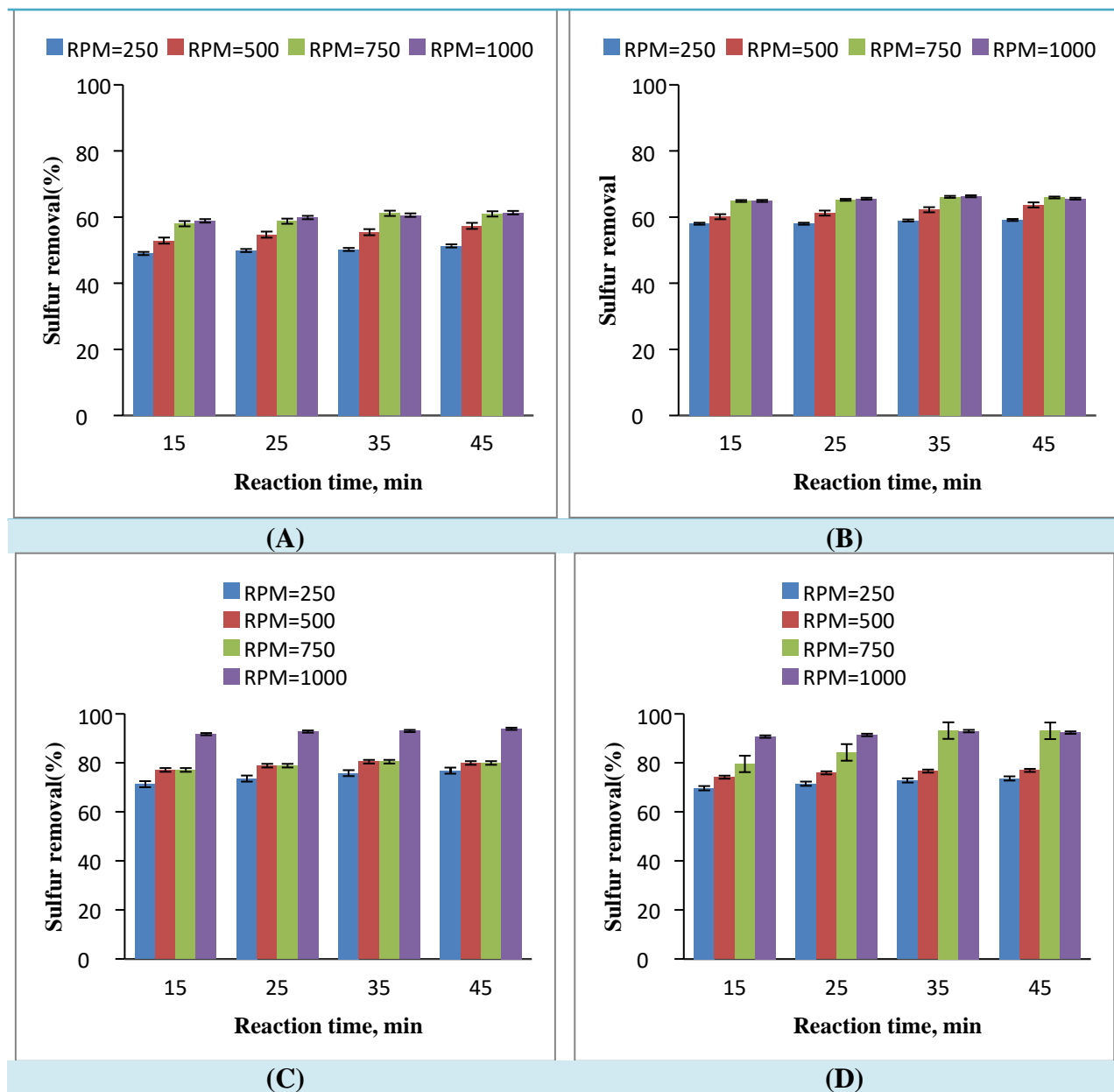


Figure 7: Effect of oxidation time for ODS performance at several speed of mixing and reaction temperature A) 40 °C, B) 60 °C, C) 80 °C and D) 100 °C using (10% MnO₂/AC-support)

3.3.3 Effect of Oxidation Temperature

The temperature effects on the oxidative desulfurization process have been studied at 40°C, 60°C, 80 °C and 100 °C utilizing different reaction times as explained in the Figure 8. In the experimental work presented in these Figures, it can be noticed that the effect of temperature on

the Oxidation performance is improved via increasing reaction temperature [16, 33]. Figure 8(a) shows the impact of increasing of oxidation temperature on sulfur conversion for reaction time of 15 min but with different speed of mixing (250, 500, 750 and 1000) rpm. Sulfur conversion improved from 59% to 90.76% when the reaction temperature is increased from 40 °C to 100 °C at speed 1000 rpm. With reaction temperature increase from 40 °C to 80 °C, the sulfur elimination has remarkably improved from 61.14% to 94.14%, with reaction time of 35 min at 750 rpm as explained in the Figure 8b. Such reaction behavior is due to the fact that enhancing the oxidation temperature improves the activation energy and as a result increases the diffusion sulfur and oxygen molecules inside the catalyst pore. Figures 8(a, b & c) represent the influence of the reaction temperature and speed of mixing on the sulfur removal from kerosene for different reaction time. It was obvious that the DBT removing activity improved via enhancing oxidation time under various oxidation temperatures. So, the oxidation temperature had greater impact on sulfur elimination compared to reaction time [23].

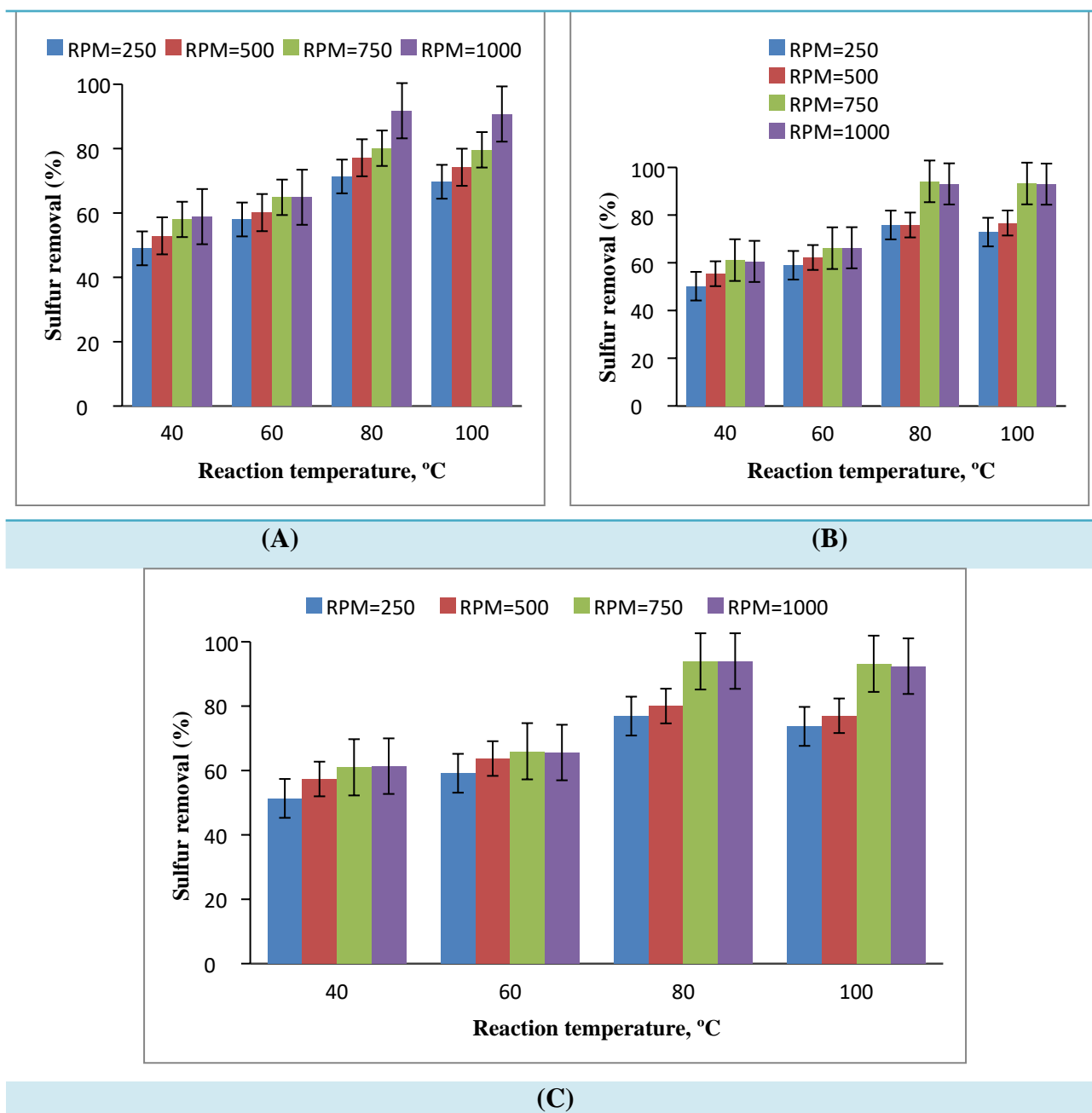


Figure 8: Temperature influence of sulfur removal at various speed of digital mixing at reaction times a) 15 min, b) 35 min and c) 45 min on ODS process

The comparison between the reactivity of the new nanocatalyst and the previous studies was explained in the Table 3:

Table 3: Comparison between the reactivity of new nano catalyst and the previous studies

Sulfur compound	oxidant/ catalyst	Sulfur removal	Reference
TH	<i>n</i> -heptane, H ₂ O ₂ /TiO ₂ /ZSM-12	60%	[34]
DBT	Diesel, H ₂ O ₂ / Fe ₂ O ₃ / AC	71%	[35]
DBT	Kerosene, MnO ₂ /SnO ₂	92.4 %	[10]
DBT	Kerosene, H ₂ O ₂ / MnO ₂ /AC	94%	Present study

3.4 Nano catalyst Deactivation and regeneration

3.4.1 Deactivation of the nano catalyst

In the present work, the new nano (10%MnO₂/AC) catalyst reactivity was examined after four ODS cycles under the best experimental parameters. The performance of DBT removal after each cycle is explained in Figure 9. According to the findings, after four ODS cycles, the nano catalyst achieved a peripheral removal in the total DBT. Under the best experimental conditions, this behavior relates to the nano catalyst's notable stability. The loss of some active sites during the recovery process may be the cause of the modest decrease in the nano catalyst's reactivity.

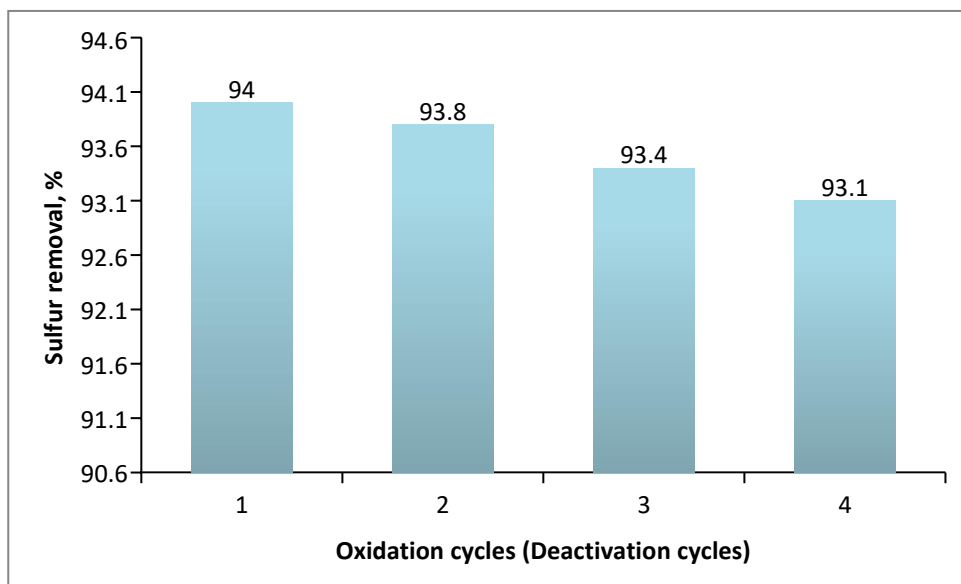


Figure 9: Recovery performance of nano (10%MnO₂/AC) catalyst for four consecutive ODS cycles at the best experimental conditions.

3.4.2 Nano catalyst Regeneration

Four ODS cycles were used to evaluate the solvent extraction regeneration (SER) process of the used nano (10%MnO₂/AC) catalyst. For regeneration technology, methanol, ethanol, and iso-octane are used as solvents. Figure 10 explained the ODS reactivity of the nanocatalyst after the regeneration technology by each used solvent. The information acquired demonstrated that regeneration activity decreases in the following order: iso-octane, ethanol, and then methanol. So, the spent nano (10%MnO₂/AC) catalyst can be excellently regenerate via employing iso-octane.

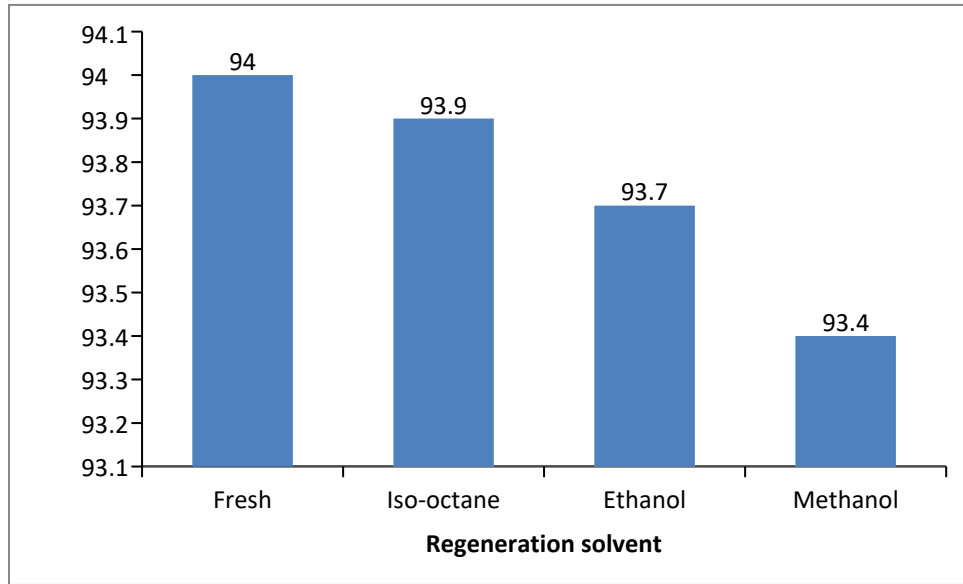


Figure 10: Regeneration performance of nano (10% MnO_2/AC) catalyst via SER process.

4. Mathematical Modeling of ODS Process in DBR

4.1 Model depending on ODS Kinetics in DBR

Pseudo first and second order kinetics is modeled here and are shown in Table 4.

Table 4: Equations used in the modeling of ODS in DBR

Parameter	Symbol	Equations/values	Eq. no.	Ref.
Reaction rate	$(-r_{DBT})$	$(-r_{DBT}) = \eta_0 * k * C_{DBT}^n$	(1)	[23]
Arrhenius equation	(k)	$k = k_0 * e^{(-\frac{EA}{RT})}$	(2)	[32, 33]
The final DBT concentration	(C_{DBT})	$C_{DBT} = [C_{DBT,t}^{(1-n)} + (n-1) * t * K_{in} * \eta_0]^{\frac{1}{1-n}}$	(3)	[34]
The effectiveness factor	(η_0)	$\eta_0 = \frac{3 * (\phi * \coth\phi - 1)}{\phi^2}$	(4)	[34, 35]
Thiele modulus	(ϕ)	$\phi = \frac{V_p}{S_p} \sqrt{\left(\frac{n+1}{2}\right) \frac{k_{in} * C_{DBT}^{(1-n)} * \rho_p}{D_{ei}}}$	(5)	[34, 35]

The catalyst effective diffusivity	(D_{ei})	$D_{ei} = \frac{\varepsilon_B}{\mathcal{J}} * \frac{1}{\frac{1}{D_{mi}} + \frac{1}{D_{ki}}}$	(6)	[23, 35]
The Knudsen diffusivity	(D_{ki})	$D_{ki} = 9700 * r_g * \left(\frac{T}{M_{wi}}\right)^{0.5}$	(7)	[23, 34]
Mean pore radius	(r_g)	$r_g = \frac{2 * V_g}{S_g}$	(8)	[36]
The molecular diffusivity	(D_{mi})	$D_{mi} = 8.93 * 10^{-8} \left(\frac{v_l^{0.267} * T}{v_{DBT}^{0.433} * \mu_l}\right)$	(9)	[37, 38]
The porosity of catalyst	(ε_B)	$\varepsilon_B = V_g * \rho_p$	(10)	[23, 35]
Particle density	(ρ_p)	$\rho_p = \frac{\rho_B}{1 - \varepsilon_B}$	(11)	[23, 35]
The tortuosity factor	(\mathcal{J})	The tortuosity factor (\mathcal{J}) of the pore network is 2 to 7	----	[39]
The molar volume of the sulfur compound	(v_{DBT})	$v_{DBT} = 0.2850 * v_{cDBT}^{1.0480}$	(12)	[40]
The external volume of the catalyst (For sphere particle)	(V_p)	$V_p = \frac{4}{3} * \pi * r_p^3$	(13)	[41]
The external surface of the synthetic catalyst as sphere particle	(S_p)	$S_p = 4 * \pi * r_p^2$	(14)	[41]
The kerosene viscosity	(μ_l)	$\mu_l = 3.1410 * 10^{10} * (T - 460.0)^{-3.4440} * (\log API)^\alpha$	(15)	[42]
Dimensionless number	(α)	$\alpha = 10.3130 * [\log_{10}(T - 460.0)] - 36.4470$	(16)	[42]
American petroleum institute	(API)	$API = \frac{141.5}{sp. gr_{15.6}} - 131.5$	(17)	[43]

4.2 Kinetic parameters estimation technique

The kinetic parameters can be evaluated employing mathematical model based techniques coupled with experimental data. To determine the optimal values kinetic parameters, the minimization of the following objective function was considered:

$$OBJ = \sum_{n=1}^{N_t} (C_{DBT}^{exp} - C_{DBT}^{pred})^2 \quad (18)$$

where, N_t is the number of experimental runs, C_{DBT}^{exp} are the experimental concentration of sulfur (DBT), and C_{DBT}^{pred} are the predicted concentration of sulfur obtained using the mathematical model.

The amount of sulfur (DBT) removal can be estimated depending on the equation as follow:

$$(X)_{DBT} = (1 - \frac{C_{DBT}}{C_{DBT,t}}) \quad (19)$$

Where:

C_{DBT} : concentration of DBT

$C_{DBT,t}$: concentration of DBT at reaction time (t)

4.3 Optimization problem formulation for evaluation of kinetic parameter

The problem of parameter estimation can be described as:

Given: Catalyst type, reactor design, and the operating conditions of ODS reaction.

Obtain: The order of reaction (n), the pre-exponential factor (k_0) and activation energy (EA) for prepared catalyst at different rpm.

So as to minimize: the sum of squared error (SSE).

Subjected to: constraints of operation.

Mathematically, the optimization problem is written as follow:

Min: **SSE**

$n^j, EA^j, k_i^j, (j = \text{rpm}, 1-4)$

$$\begin{aligned}
\text{S.t.} \quad & f(z, x(z), \dot{x}(z), u(z), v) = 0 \\
& C_L \leq C \leq C_U \\
& n_L^j \leq n^j \leq n_U^j \\
& EA_L^j \leq EA^j \leq EA_U^j \\
& k_{oL}^j \leq k_i^j \leq k_{oU}^j
\end{aligned}$$

$f(z, x(z), \dot{x}(z), u(z), v) = 0$: represent the ODS technology model.

z : is independent variable.

$u(z)$: is the decision variable.

$x(z)$: represent the set of all variables.

$\dot{x}(z)$: represent the derivative of the variables with respect to time.

v : is the design variable.

C_L, C_U : lower and upper bounds of concentration.

L, U : are lower and upper bounds.

rpm, 1-4: revolutions per minute

5. Results

5.1 Kinetic parameters

The constant parameters used in the kinetic parameter estimation are presented in Table 5. The optimal values of the kinetic parameters obtained via the mathematical optimization process are displayed in Tables 6 to 9.

Table 5: Values of constant parameters used in the modeling operation of ODS

Parameter, unit	Value
Initial concentration of DBT compounds (Ct), ppm	543
Oxidation time, min	15, 25, 35, 45
Reaction temperature (T ₁ , T ₂ , T ₃) °C	40, 60, 80
Density of fuel at 15 °C, gm/cm ³	0.7845
T _{meABP} , °R	756.0
Acceleration gravity (g), m/sec ²	9.81
R, J/mole.°K	8.3140
Vg, cm ³ /gm	0.4536
Sg, cm ² /gm	7073700
Vp, cm ³	0.0114
Sp, cm ²	0.283
ρ _B , gm/cm ³	1.794
M.Wt of fuel (M _{wL}), gm/mole	170.0
M.Wt of DBT (Mwi), gm/mole	184.0
r _g , nm	1.282

Table 6: Optimal model parameters at 250 rpm

Parameter	Value	Unit
n	1.993359	–
EA	28.318	KJ/mol.
k _o	41452.48	
SSE	1.41158 × 10 ⁻⁵	–

Table 7: Optimal model parameters at 500 rpm

Parameter	Value	Unit
n	1.938691	–
EA	27.617	KJ/mol.
k_0	42131.69	
SSE	1.21119×10^{-5}	–

Table 8: Optimal model parameters at 750 rpm

Parameter	Value	Unit
n	1.837157	–
EA	25.477	KJ/mol.
k_0	38730.30	
SSE	3.87686×10^{-6}	–

Table 9: Optimal model parameters at 1000 rpm

Parameter	Value	Unit
n	1.86807	–
EA	25.8360	KJ/mol.
k_0	46142.42	
SSE	4.84172×10^{-6}	–

Based on the obtained results in Tables 5 to 8, it is observed that the order of ODS reactions (n) and activation energy (EA) were decreased with increasing the mixing rate from 250 RPM to 1000 RPM. The increasing in the mixing rate was improved the performance of ODS process by making the reaction more fast and this agreement with the values of reaction order which

approached from one with increasing RPM. Also, the required activated energy was decreased with increasing the mixing rate due to increasing RPM generated efficient mixture which required lower activation energy of molecules for completing the reactions. The low value of EA at 1000 RPM proved that the catalytic ODS process was more efficient, and the oxidation of DBT is faster [48, 49]. The oxidation performance of the kerosene was increased with the enhancing in the electron density of the sulfur compounds and led to decrease EA of ODS process [50, 51]. So, the low EA can be returned to the electrophilic addition of oxygen or the large electron density on sulfur atom in DBT compound [52]. The low EA also can be driving force compel the DBT which was thermally less staggered for reacting with the oxidant, and improved the oxidation reactions [53].

5.2 Experimental and simulation results

The data obtained experimentally and predictably at various reaction temperature, reaction time and mixing speed are explained in Tables 8, 9, and S2 to S5. As illustrated in these Tables, the values of kinetic parameters obtained by mathematical modeling process result in low error (<5%). Also, Figures 11 to 14 show the difference between the experimental and predicted results. Based on the results, an excellent agreement between the experimental and predicted values is obtained under the same process conditions. The correlation between these data explains to be straight line with a slope close approximately to 1.0, which shows a dramatic agreement between it.

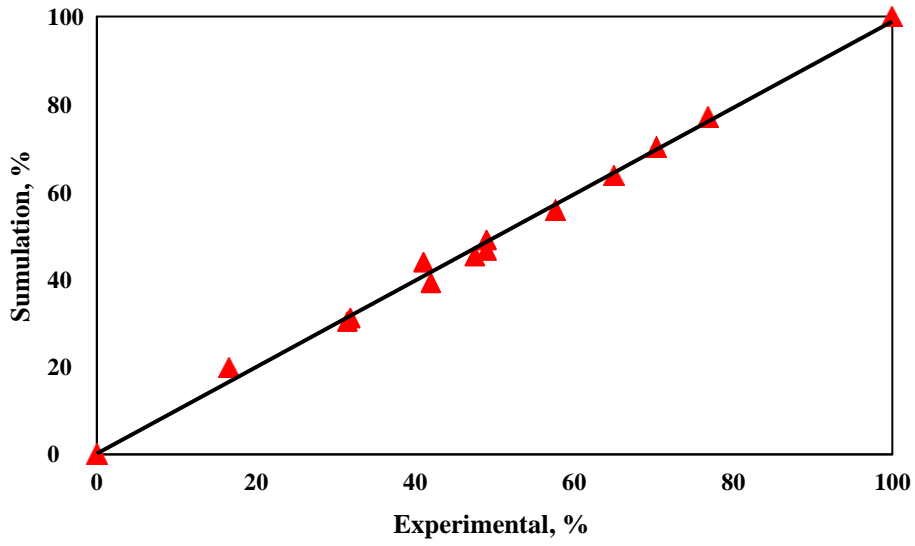


Figure 11: Experimental data in comparing to simulated data at 250 rpm

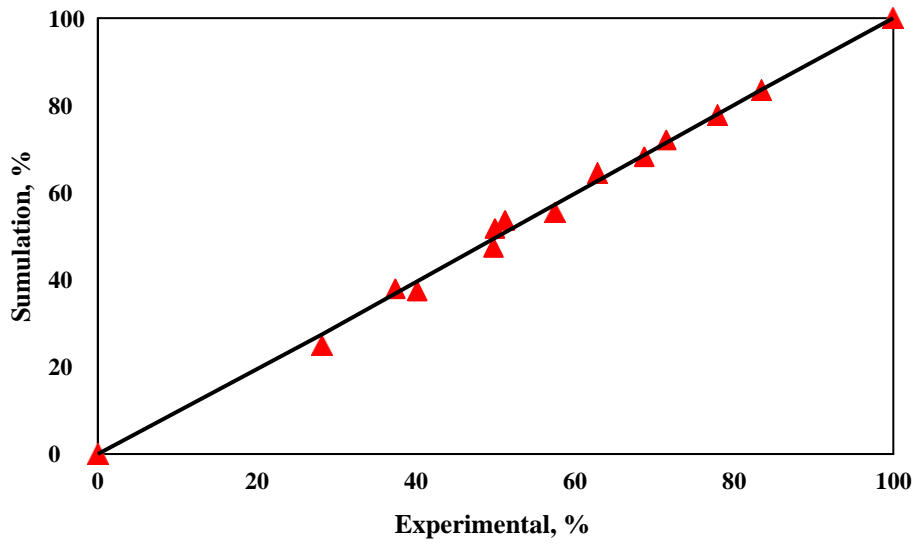


Figure 12: Experimental data in comparing to simulated data at 500 rpm

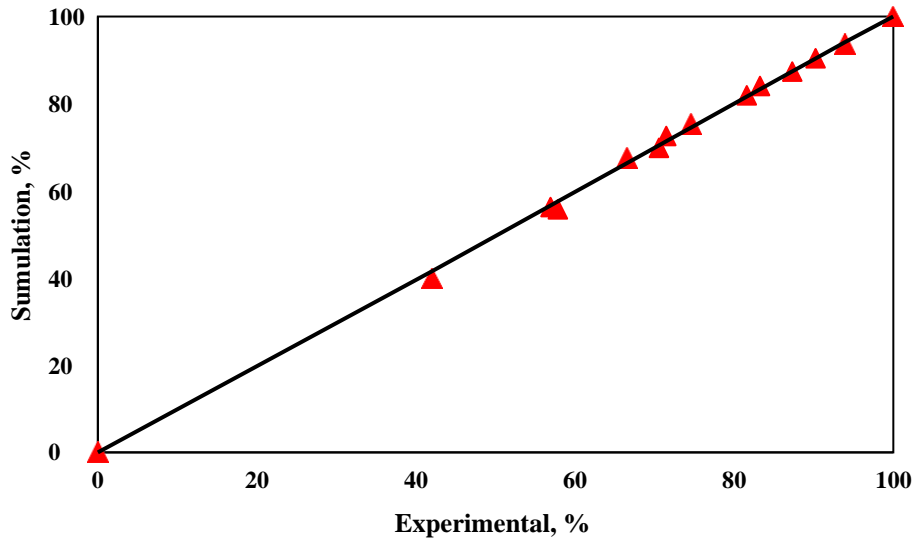


Figure 13: Experimental data in comparing to simulated data at 750 rpm

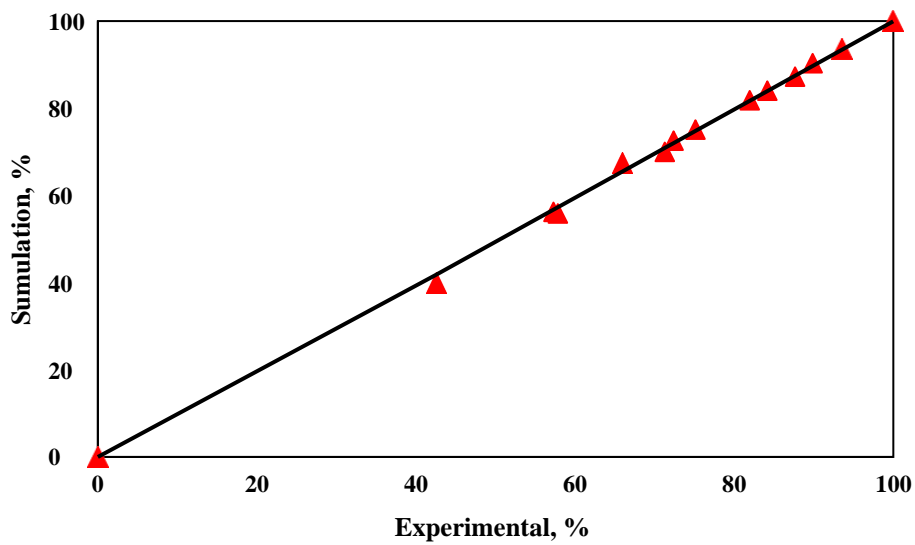


Figure 14: Experimental data in comparing to simulated data at 1000 rpm

6. Maximizing of sulfur removal

6.1 Formulation of optimization problem

The kinetic parameters estimated earlier are utilized to optimize the ODS conditions while maximizing the performance of sulfur elimination. The optimization problem can be explained as:

Given: The reactor configuration, the reaction order, the catalyst and pre-exponential factor and activation energy for the reaction.

Optimize: The operating parameters such as reaction time and reaction temperature for high conversion.

So as to maximize: The sulfur removal from the kerosene fuel.

Subjected to: Process constraints

The problem is represented mathematically as follows:

Max

$j = \text{RPM-1, 2, 3, 4}$

$$\begin{aligned} \text{S.t.} \quad & f(z, x(z), \dot{x}(z), u(z), v) = 0 && \text{(process model)} \\ & && \leq \leq \\ & && \leq \leq \\ & && \leq \leq \\ & && \leq \leq \end{aligned}$$

Where:

C_{DBT} : initial concentration of DBT

$C_{\text{DBT},t}$: concentration of DBT at reaction time (t)

$X_{\text{DBT}, t}$: conversion of DBT at reaction time (t)

$f(z, x(z), \dot{x}(z), u(z), v) = 0$: represent the ODS technology model

z : is independent variable.

$u(z)$: is the decision variable.

$x(z)$: represent the set of all variables.

$\dot{x}(z)$: represent the derivative of the variables with respect to time.

v : is the design variable.

$C_{\text{DBT},L}, C_{\text{DBT},U}$: lower and upper bounds of concentration.

$\text{Time}_L, \text{Time}_U$: lower and upper bounds of time.

$X_{\text{DBT},L}, X_{\text{DBT},U}$: time , lower and upper bounds of conversion.

The optimization process is conducted via gPROMS software.

6.2 Optimum operating conditions for maximizing sulfur removal

The optimal operating conditions for each mixing speed are presented in Table 10.

Table 10: Optimal values of ODS technology conditions

Parameter, unit	Values			
	rpm-1	rpm-2	rpm-3	rpm-4
, ppm	539	534	535	544
T, °C	73	68	66	74
Time, min	200	200	152	123
Sulfur Conversion, %	96.1	97.4	99.1	99

Depending on the data showed in Table 10, the highest sulfur removal efficiency of sulfur compound was 96.1%, 97.4%, 99%, and 99.1% which carried out by employing 10%Mn/Nano-AC at (539 ppm, 73 °C, 200 min), (535 ppm, 68 °C, 200 min), (544 ppm, 74 °C, 152 min), and (535 ppm, 66 °C, 123 min) respectively to match the environmental regulations to obtain almost eco-friendly fuel. The optimization data proved that the optimal operating conditions (535 ppm, 66 °C, and 123 min) made significant effect to obtain (535 ppm, 66 °C, 123 min) the higher sulfur removal efficiency (99.1 %). Therefore, high quality fuel was regarded the main goal of the present work. From the data in Table 13 shows that under certain conditions the ODS process using of the nano-catalyst and the reactor designed in this study results in greener fuel in terms of sulfur content.

7. Conclusions

In this study, oxidative desulfurization process was carried out using new metal oxide over Nano-activated carbon particles (10%Mn/ Nano-AC) catalyst and a novel digital basket reactor (DBR) for producing high quality kerosene fuel. The performance of the oxidation reactions under mild operating conditions has been improved utilizing the new reactor and nano-catalyst investigated here. The new homemade nano catalyst prepared in this study has been characterized by SEM, EDX, BET, and FTIR tests and an efficient catalyst was achieved. The experimental data proved that the new nano-catalyst in the new DBR design generated satisfactory sulfur conversion (94.149%) under oxidation temperature of 80 °C, oxidation time of 35 min and agitation rate of 750 rpm. The catalyst reactivity was tested after four consecutive ODS cycles under the best experimental parameters and the used catalyst showed excellent stability in terms of DBT removal efficiency. The spent catalyst was treated by methanol, ethanol and iso-octane solvents for regenerated it, and the result proved that iso-octane carried out the maximum regeneration performance. An optimization technique according to the minimization of the sum of the squared error between the data obtained experimentally and predicted by model of the new ODS process was employed to evaluate the optimal kinetic parameters of the desulfurization process. The ODS process model was able to predict the experimental data for a wide range of conditions very well via absolute average < than 5%.

Nomenclature

D_{mi}	Molecular diffusivity
Sp. gr _{15.6}	Specific gravity of kerosene at 15.6°C
M_{WL}	Liquid molecular weight of kerosene
M_{wi}	Molecular weight of DBT
R	Gas constant
$-r_{DBT}$	Reaction rate of DBT
r_g	Pore radius (nm)
r_p	Particle radius
S_p	External surface area of catalyst particle
S_g	Specific surface area of particle
V_p	External Volume of catalyst particle
V_g	Pore volume
T_{meABP}	Mean average boiling point

Greek Symbols

η_0	Effectiveness factor
Φ	Thiel modulus
\mathcal{E}_B	Porosity
\mathcal{J}	Tortuosity
ρ_B	Bulk density
ρ_p	Particle density
$\rho_{L15.6}$	Density of kerosene at 15.6°C(gm/cm ³).
μ_l	Viscosity of liquid
v_l	Liquid molar volume
v_{cl}	Critical molar volume of liquid

v_{DBT}	Molar volume of DBT
v_{cDBT}	Critical volume of DBT compound.
0	Initial (at time = 0)

References

- Humadi, J. I., Gheni, S. A., Ahmed, S. M., Abdullah, G. H., Phan, A. N., & Harvey, A. P., Fast, non-extractive, and ultradeep desulfurization of diesel in an oscillatory baffled reactor. *Process Safety and Environmental Protection*, 2021. *152*, 178-187.
- Jafar, S.A., A.T. Nawaf, and J.I. Humadi, *Improving the extraction of sulfur-containing compounds from fuel using surfactant material in a digital baffle reactor*. *Materials Today: Proceedings*, 2021. **42**: p. 1777-1783.
- Sarda, K. K., Bhandari, A., Pant, K. K., & Jain, S., Deep desulfurization of diesel fuel by selective adsorption over Ni/Al₂O₃ and Ni/ZSM-5 extrudates. *Fuel*, 2012. *93*, 86-91.
- Armstrong, S.M., B.M. Sankey, and G. Voordouw, *Evaluation of sulfate-reducing bacteria for desulfurizing bitumen or its fractions*. *Fuel*, 1997. **76**(3): p. 223-227.
- Aabid, A. A., Jafar, S. A., Ahmed, M. O., & Humadi, J. I., Inhibitory effect of ceftriaxone sodium on corrosion of copper in 1M nitric acid. *Materials Today: Proceedings*, 2021.
- Jafar, S.A., A.A. Aabid, and J.I. Humadi, *Corrosion behavior of carbon steel in 1 M, 2 M, and 3 M HCl solutions*. *Materials Today: Proceedings*, 2022. **57**: p. 412-417.
- Jafar, S. A., Aabid, A. A., Razzaq, G. H. A., & Humadi, J. I., Sodium nitrate as a corrosion inhibitor of carbon steel in various concentrations of hydrochloric acid solution. *Journal of New Materials for Electrochemical Systems*, 2022. *25*(1), 32-37.
- Humadi, J. I., Gheni, S. A., Ahmed, S. M., & Harvey, A., Dimensionless evaluation and kinetics of rapid and ultradeep desulfurization of diesel fuel in an oscillatory baffled reactor. *RSC Advances*, 2022. *12*(23), 14385-14396.
- Qian, E.W., *Development of Novel Nonhydrogenation Desulfurization Process—Oxidative Desulfurization of Distillate—*. *Journal of the Japan petroleum institute*, 2008. **51**(1): p. 14-31.
- Humadi, J. I., Issa, Y. S., Aqar, D. Y., Ahmed, M. A., Alak, H. H. A., & Mujtaba, I. M., Evaluation the performance of the tin (IV) oxide (SnO₂) in the removal of sulfur compounds via oxidative-extractive desulfurization process for production an eco-friendly fuel. *International Journal of Chemical Reactor Engineering*, 2022.
- Jarullah, A.T., I.M. Mujtaba, and A.S. Wood, *Kinetic parameter estimation and simulation*

- of trickle-bed reactor for hydrodesulfurization of crude oil*. Chemical engineering science, 2011. **66**(5): p. 859-871.
12. Braunschweig, B. and X. Joulia, *18th European symposium on computer aided process engineering*. 2008: Elsevier.
 13. Al-Malki, A., *Desulfurization of gasoline and diesel fuels, using non-hydrogen consuming techniques*. 2004, King Fahd University of Petroleum and Minerals (Saudi Arabia).
 14. Palaić, N., Sertić-Bionda, K., Margeta, D., & Podolski, Š., *Oxidative desulphurization of diesel fuels*. Chemical and Biochemical Engineering Quarterly, 2015. **29**(3): p. 323-327.
 15. Zhou, X., Zhao, C., Yang, J., & Zhang, S., *Catalytic oxidation of dibenzothiophene using cyclohexanone peroxide*. Energy & fuels, 2007. **21**(1): p. 7-10.
 16. García-Gutiérrez, J. L., Fuentes, G. A., Hernandez-Teran, M. E., Garcia, P., Murrieta-Guevara, F., & Jiménez-Cruz, F., *Ultra-deep oxidative desulfurization of diesel fuel by the Mo/Al₂O₃-H₂O₂ system: The effect of system parameters on catalytic activity*. Applied Catalysis A: General, 2008. **334**(1-2): p. 366-373.
 17. Arcibar-Orozco, J.A., J.R. Rangel-Mendez, and T.J. Bandosz, *Desulfurization of model diesel fuel on activated carbon modified with iron oxyhydroxide nanoparticles: effect of tert-butylbenzene and naphthalene concentrations*. Energy & fuels, 2013. **27**(9): p. 5380-5387.
 18. Yan, X. M., Mei, P., Xiong, L., Gao, L., Yang, Q., & Gong, L., *Mesoporous titania-silica-polyoxometalate nanocomposite materials for catalytic oxidation desulfurization of fuel oil*. Catalysis Science & Technology, 2013. **3**(8): p. 1985-1992.
 19. Fraile, J. M., Gil, C., Mayoral, J. A., Muel, B., Roldán, L., Vispe, E., & Puente, F., *Heterogeneous titanium catalysts for oxidation of dibenzothiophene in hydrocarbon solutions with hydrogen peroxide: On the road to oxidative desulfurization*. Applied Catalysis B: Environmental, 2016. **180**: p. 680-686.
 20. Nawaf, A. T., Jarullah, A. T., Gheni, S. A., & Mujtaba, I. M., *Development of kinetic and process models for the oxidative desulfurization of light fuel, using experiments and the parameter estimation technique*. Industrial & Engineering Chemistry Research, 2015. **54**(50): p. 12503-12515.
 21. Ma, X., Sakanishi, K., Isoda, T., & Mochida, I., *Quantum chemical calculation on the desulfurization reactivities of heterocyclic sulfur compounds*. Energy & Fuels, 1995. **9**(1): p. 33-37.

22. Ahmed, G.S., J.I. Humadi, and A.A. Aabid, *Mathematical Model, Simulation and Scale up of Batch Reactor Used in Oxidative Desulfurization of Kerosene*. Iraqi Journal of Chemical and Petroleum Engineering, 2021. **22**(3): p. 11-17.
23. Nawaf, A.T., A.T. Jarullah, and L.T. Abdulateef, *Design of a synthetic zinc oxide catalyst over nano-alumina for sulfur removal by air in a batch reactor*. Bulletin of Chemical Reaction Engineering & Catalysis, 2019. **14**(1): p. 79-92.
24. Yadav, B.R. and A. Garg, *Performance assessment of activated carbon supported catalyst during catalytic wet oxidation of simulated pulping effluents generated from wood and bagasse based pulp and paper mills*. RSC advances, 2017. **7**(16): p. 9754- 9763.
25. Chen, J., Peng, J., He, A., Gao, L., Omran, M., & Chen, G., *Investigation on the decomposition of titanium slag using sodium carbonate for preparing rutile TiO₂*. Materials Chemistry and Physics, 2022. **290**: p. 126626.
26. Yacob, A. R., Mustapha, N. M., Mustajab, K. A., & Al-Swaidan, H. M., *Physical activation of Saudi Arabia date palm tree's foliar, frond and thorn*. in *2010 International Conference on Mechanical, Industrial, and Manufacturing Technologies*. 2010.
27. Kalderis, D., Bethanis, S., Paraskeva, P., & Diamadopoulou, E., *Production of activated carbon from bagasse and rice husk by a single-stage chemical activation method at low retention times*. Bioresource technology, 2008. **99**(15): p. 6809-6816.
28. Hayashi, J. I., Horikawa, T., Takeda, I., Muroyama, K., & Ani, F. N., *Preparing activated carbon from various nutshells by chemical activation with K₂CO₃*. Carbon, 2002. **40**(13): p. 2381-2386.
29. Watari, T., Tsubira, H., Torikai, T., Yada, M., & Furuta, S., *Preparation of porous carbon/silica composites from rice husk powder*. Journal of Ceramic Processing & Research, 2003. **4**(4): p. 177-180.
30. Kuśmierk, K. and A. Świątkowski, *The influence of different agitation techniques on the adsorption kinetics of 4-chlorophenol on granular activated carbon*. Reaction Kinetics, Mechanisms and Catalysis, 2015. **116**(1): p. 261-271.
31. Shihab, M. A., Nawaf, A. T., Mohamedali, S. A., & Alsalmaney, M. N., *Improving porosity of activated carbon nanotubes via alkali agents for the enhancement of adsorptive desulfurization process*. in *Materials Science Forum*. 2020. Trans Tech Publ.

32. Abdulateef, L. T., Nawaf, A. T., Al-Janabi, O. Y. T., Foot, P. J., & Mahmood, Q. A., *Batch Oxidative Desulfurization of Model Light Gasoil over a Bimetallic Nanocatalyst*. Chemical Engineering & Technology, 2021. **44**(9): p. 1708- 1715.
33. Nawaf, A. T., Gheni, S. A., Jarullah, A. T., & Mujtaba, I. M., *Optimal design of a trickle bed reactor for light fuel oxidative desulfurization based on experiments and modeling*. Energy & Fuels, 2015. **29**(5): p. 3366-3376.
34. Santos, M.R.F.d., A.M.G. Pedrosa, and M.J.B.d. Souza, *Oxidative desulfurization of thiophene on TiO₂/ZSM-12 zeolite*. Materials Research, 2016. **19**: p. 24-30.
35. Ugal, J. R., Jima'a, R. B., Al-Jubori, W. M. K., Bayader, F. A., & Al-Jubori, N. M., *Oxidative desulfurization of hydrotreated gas oil using Fe₂O₃ and Pd loaded over activated carbon as catalysts*. Oriental journal of chemistry, 2018. **34**(2): p. 1091.
36. Huang, P., Luo, G., Kang, L., Zhu, M., & Dai, B., *Preparation, characterization and catalytic performance of HPW/aEVMcatalyst on oxidative desulfurization*. RSC advances, 2017. **7**(8): p. 4681-4687.
37. Saha, B., S. Kumar, and S. Sengupta, *Green synthesis of nano silver on TiO₂ catalyst for application in oxidation of thiophene*. Chemical Engineering Science, 2019. **199**: p. 332-341.
38. Ahmed, G. S., Jarullah, A. T., Al-Tabbakh, B. A., & Mujtaba, I. M., *Design of an environmentally friendly reactor for naphtha oxidative desulfurization by air employing a new synthetic nano-catalyst based on experiments and modelling*. Journal of cleaner production, 2020. **257**: p. 120436.
39. Jarullah, A. T., Ahmed, G. S., Al-Tabbakh, B. A., & Mujtaba, I. M., *Enhancement of light naphtha quality and environment using new synthetic nano-catalyst for oxidative desulfurization: Experiments and process modeling*. Computers & Chemical Engineering, 2020. **140**: p. 106869.
40. Nawaf, A. T., Jarullah, A. T., Hameed, S. A., & Mujtaba, I. M., *Design of new activated carbon based adsorbents for improved desulfurization of heavy gas oil: experiments and kinetic modeling*. Chemical Product and Process Modeling, 2021. **16**(3): p. 229-249.
41. Paraskos, J., J. Frayer, and Y. Shah, *Effect of holdup incomplete catalyst wetting and backmixing during hydroprocessing in trickle bed reactors*. Industrial & Engineering Chemistry Process Design and Development, 1975. **14**(3): p. 315-322.
42. Duduković, M.P., F. Larachi, and P.L. Mills, *Multiphase catalytic reactors: a perspective on current knowledge and future trends*. Catalysis reviews, 2002. **44**(1): p. 123-246.

43. Jarullah, A. T., Aldulaimi, S. K., Al-Tabbakh, B. A., & Mujtaba, I. M., *A new synthetic composite nano-catalyst achieving an environmentally Friendly fuel by batch oxidative desulfurization*. Chemical Engineering Research and Design, 2020. **160**: p. 405-416.
44. Zakrzewska, I. and A. Samochowiec, *Characteristics of selected traits of Adult Children of Alcoholics in the context of their parents' attitudes*. Current Problems of Psychiatry, 2017. **18**(4).
45. Al-Huwaidi, J. S., Al-Obaidi, M. A., Jarullah, A. T., Kara-Zaitri, C., & Mujtaba, I. M., *Modeling and simulation of a hybrid system of trickle bed reactor and multistage reverse osmosis process for the removal of phenol from wastewater*. Computers & Chemical Engineering, 2021. **153**: p. 107452.
46. Ahmed, T., *Hydrocarbon phase behavior*. 1989.
47. Poyton, A. A., Varziri, M. S., McAuley, K. B., McLellan, P. J., & Ramsay, J. O., *Parameter estimation in continuous-time dynamic models using principal differential analysis*. Computers & chemical engineering, 2006. **30**(4): p. 698- 708.
48. Ahmad, W. and I. Ahmad, *Desulphurization of transportation fuels by per-formic acid oxidant using MoOx loaded on ZSM-5 catalyst*. Journal of Power and Energy Engineering, 2017. **5**(12): p. 87-99.
49. Ibrahim, N.K., W.A. Noori, and J.M. Khasbag, *Ultrasound-Assisted Oxidative Desulfurization of Diesel*. Journal of Engineering, 2016. **22**(11): p. 55-67.
50. Sachdeva, T. and K. Pant, *Deep desulfurization of diesel via peroxide oxidation using phosphotungstic acid as phase transfer catalyst*. Fuel Processing Technology, 2010. **91**(9): p. 1133-1138.
51. Ahmad, W., I. Ahmad, and M. Yaseen, *Desulfurization of liquid fuels by air assisted peracid oxidation system in the presence of Fe-ZSM-5 catalyst*. Korean Journal of Chemical Engineering, 2016. **33**(9): p. 2530-2537.
52. Hasan, Z., J. Jeon, and S.H. Jhung, *Oxidative desulfurization of benzothiophene and thiophene with WOx/ZrO2 catalysts: effect of calcination temperature of catalysts*. Journal of hazardous materials, 2012. **205**: p. 216-221.
53. Borah, D., *Desulfurization of organic sulfur from a subbituminous coal by electron-transfer process with K4 [Fe (CN) 6]*. Energy & fuels, 2006. **20**(1): p. 287-294.